UNIVERSITÀ DI SIENA 1240

USiena

The potential impacts of plastic on the marine carbon cycle

This is the peer reviewed version of the following article:

Original:

Pang, Q., Wu, P., Galgani, L., Wang, X., Zhang, Z., Yuan, T., et al. (2025). The potential impacts of plastic on the marine carbon cycle. NATURE SUSTAINABILITY, 8(10), 1154-1163 [10.1038/s41893-025-01632-7].

Availability:

This version is availablehttp://hdl.handle.net/11365/1330420 since 2026-10-29T15:23:53Z

Published:

DOI: http://doi.org/10.1038/s41893-025-01632-7

Terms of use:

Open Access

The terms and conditions for the reuse of this version of the manuscript are specified in the publishing policy. Works made available under a Creative Commons license can be used according to the terms and conditions of said license.
For all terms of use and more information see the publisher's website.

(Article begins on next page)

16 November 2026

The Potential Impacts of Plastic on the Marine Carbon Cycle

Qiaotong Pang[1], Peipei Wu[2], Luisa Galgani[3,4], Xinle Wang[1], Ziman Zhang[1], Tengfei Yuan[5], Haikun Wang[1], Yanxu Zhang[5*]

[1]School of Atmospheric Sciences, Nanjing University, Jiangsu, China

[2]Scripps Institution of Oceanography, University of California San Diego, La Jolla, California, USA

[3]Environmental Spectroscopy Group, Department of Biotechnology, Chemistry and Pharmacy, University of Siena, Italy

[4]National Biodiversity Future Center, Palermo, Italy

[5]Department of Earth and Environmental Science, Tulane University, New Orleans, Louisiana, USA

[*]Corresponding author: yzhang127@tulane.edu

Abstract

Increasing plastic waste has triggered global concerns for the potential detrimental effects on marine ecosystems. The impact of plastic reaches beyond the immediate harm to marine life to encompass the marine biogeochemical cycle and the global carbon budget. We investigate these effects by integrating an oceanic plastic simulation with a marine ecosystem model. We find that oceanic plastic could disturb the marine carbon cycle through three pathways: the plastic carbon buried in sediments, the release of dissolved organic carbon from water-column plastic, and the toxicity effect on marine phytoplankton. Our scenario analysis suggests there are 0.70 (0.13 - 3.8) Tg of plastics entering the ocean every year, however, the overall impact of oceanic plastics on decreasing ocean carbon uptake could reach 12.1 TgC yr^{-1}. Our model predicts that the global plastic released into the ocean could result in up to 1.6 PgC of lost ocean carbon uptake and storage by 2050, given the foreseeable growth of plastic production and its long-lasting impacts. We urge comprehensive control policies to mitigate the losses caused by marine plastics both in ecosystem integrity and addressing climate change.

Main Text

The rampant consumption of plastics has raised concerns about the sustainable future of the world due to the immense volumes of plastic waste and the diverse damages they inflict on various environments. The ocean, in particular, is significantly affected, with millions of metric tons of plastic waste entering through various pathways, including river transport, atmospheric deposition, shipping, fishing activities, and beach littering[1,2]. Plastic wastes disperses horizontally and vertically throughout the ocean, driven by the interplay of buoyancy, gravity, wind, and ocean currents[3,4]. Oceanic plastics pose threats to marine life, including entanglement of sea turtles, the asphyxiation of seabirds, and the toxic impacts on fishes[5]. Plastic pollution also affects marine microorganisms and the carbon cycle, further complicating our efforts to achieve sustainable development goals concerning plastics[6]. However, the pattern and magnitude of these impacts as well as their overall effect on the ocean and the world remain yet to be clearly quantified and understood.

The ocean, as the largest carbon reservoir, contains diverse forms of organic and inorganic carbon distributed in sediments, marine organisms, and seawater[7,8]. Under the combined effects of ocean currents and the plastic-biomass-aggregation, oceanic plastics embedded into marine snow can sink at rate of 1.4 to 152 meters per day[9]. The sinking rate is not only influenced by the density of plastics but also by the density of plastic-biomass-aggregates[10,11]. A considerable amount of carbon is buried in the marine system, such as 200 TgC yr^{-1} in marine sediments, 200 to 350 TgC yr^{-1} in coastal sediments, as well as 74.4 to 124.2 Tg of organic carbon sequestrated by the blue carbon system every year[12–14]. The sinking of biofouled plastics and non-biofouled plastics can add an additional 7.8 TgC to the ocean and coasts sediments every year[15]. Meanwhile, the remaining plastics could continuously release dissolved organic carbon (DOC) which can be utilized by marine microorganisms and directly incorporated into the marine carbon cycle[14].

Plastics could alter the grazing behavior of zooplankton, impacting the phytoplankton biomass and carbon uptake, as suggested by previous studies[15,16]. Laboratory studies, often conducted at plastic concentrations higher than marine ones, suggest that plastics could also directly impact marine phytoplankton by increasing oxidative stress, altering cell morphology, and diminishing chlorophyll levels[17,18]. These combined effects result in inhibited growth and photosynthesis of phytoplankton because of toxicity effects of plastics on plankton cells[19,20]. The extent of such impairments varies depending on the plastics composition, phytoplankton species, and phytoplankton growth characteristics[18,20–26], with the global impact remaining unknown. Given the pivotal role phytoplankton plays in supporting the whole marine ecosystem by supplying oxygen and nutrition, we propose that the cumulative growth impairments experienced by individual phytoplankton have the potential to alter the ocean biogeochemistry and carbon cycles including the uptake of CO_2.

Here, we develop a coupled ocean plastic and marine ecosystem model to assess the comprehensive impacts of oceanic plastics on the marine phytoplankton community and the carbon cycle as illustrated in Figure. 1. We use a global ocean plastic simulation

based on a three-dimensional model (NJU-MP)[1]. This model provides a detailed and comprehensive simulation of the behaviors of plastic particles in the ocean, accounting for variations in chemical compositions and sizes, including processes such as sinking, rising, drifting, beaching, and biofouling. Furthermore, it evaluates the uncertainties associated with these processes using an ensemble model approach. The model also assimilates available surface ocean plastic observations and considers the uncertainty associated with different plastic discharge inventories. The model performs reasonably well in simulating oceanic plastic concentrations, with an R^2 value of 0.38 and a root mean square error of 0.53 with a unit of log (g km^{-2}) when comparing modeled and observed surface oceanic plastic mass concentrations[1]. We use the simulated plastic distribution in the global ocean, based on emissions accumulated from 1950 to 2020, as input for marine ecosystem modeling. We examine the comprehensive impact of plastics such as DOC releasing and toxicity effects on marine phytoplankton by using the Darwin ecosystem model, which simulates interactions between marine plankton community and nutrients (e.g., carbon, nitrogen, phosphorus, silica, iron, and related compounds).[7,25]. It incorporates the growth, grazing, and mortality of different plankton functional groups (including *Diatom*, *Other large*, *Prochlorococcus, Synechococcus, Coccolithophore, and Diazotrophs*) and reproduces observed global ocean plankton community structure. We include plastic-released DOC as a new DOC source and adjust phytoplankton growth rates based on the toxicity relationship between plastics and phytoplankton in the model. Subsequently, these impacts are translated into changes in CO_2 flux from the sea to the air, and we account for the contribution of oceanic plastic waste into the global carbon budget. Given that our simulations are jointly driven by multiple results and parameters related to interactions between oceanic plastics, marine ecosystems, and marine biogeochemical cycles, we have designed various scenarios to address the range of uncertainties. We evaluate oceanic plastics' negative impacts based on results from all scenarios and discuss potential strategies to mitigate these impacts.

Plastic carbon buried in sediments and beaches Our model suggests that buried oceanic plastics could be stored in ocean sediments and beaches, which are relatively stable but non-reactive in the marine biogeochemical cycle and do not remove from the contemporary atmospheric carbon pool[6]. By modeling the spatial distribution of oceanic plastic in both sediments and beaches, we find that approximately 0.13 Tg and 0.21 Tg of carbon are buried in sediments and beaches in 2020 in our Plastic Abundance scenario (Middle) (See Methods for more details about scenarios setting), respectively (0a and 0b). The sedimentary process of oceanic plastics in our model is driven by the sinking process, and affected by the biofouling process that alters plastics' densities (See Methods). Although the sinking and storage of plastics in sediments are not part of the ocean plankton biological pump, plastics and particulate organic matters such as marine snow can combine together and mutually affect their sink processes[6,10]. Sediments shallower than 100 m receive more than 75% of the total sedimented plastic fluxes (0d). The simulated buried carbon from sedimented plastics is higher in the nearshore water areas with shallow depth and high plastic emission from land, such as the East and Southeast coasts, the high latitude Atlantic and the Arctic (0a). Similarly,

beached plastics are predominantly found in nearshore regions with higher plastic emissions, such as the populated mid-latitude regions (0b). Favorable beach morphology, especially gentle nearshore slopes and sandy coasts facilitates the beaching of oceanic plastics, leading to significant increase of buried carbon in the Caribbean Sea as well as in the Southeast Asian Seas[28].

We find that the buried carbon from oceanic plastics is affected by polymer types, encompassing which vary in density and carbon content. Our simulation includes five polymer types: PE (polyethylene), PP (polypropylene), PVC (polyvinyl chloride), PS (polystyrene), and ABS (acrylonitrile butadiene styrene plastic). These polymers represent more than 61% of global plastic production up to 2015, with the exception of ABS[29]. The contribution of different polymers to buried carbon closely mirrors their emission levels (0c). Specifically, PE and PP are the leading polymer in global plastic production, usage, and wastes[29], which contribute 32% and 25% to total sedimented and beached plastics and 35% and 28% of buried plastic carbon, respectively. Plastics with a relatively high density such as PVC (1.38 g cm^{-3}) and PS (1.05 g cm^{-3}) exhibit faster sinking velocities, leading to their higher contributions to the total sedimented and beached plastics (22% and 15%, respectively) compared to their emissions (5% and 6%, respectively)[29]. However, PVC's contribution to the buried carbon is sharply reduced (11%), attributable to its lower carbon content compared with other polymer types.

Released DOC from seawater plastic Our simulation reveals that oceanic plastics could disrupt the marine carbon cycle by releasing 0.25 TgC yr^{-1} of DOC into the global ocean (based on modeling results of 2020), which is around 63% of Romera-Castillo et al.'s estimation[14]. We incorporate a plastic-DOC release process mediated by solar radiation in the ocean ecosystem model (see Methods). In general, the distribution of plastic-released DOC mirrors the spatial patterns of seawater plastics (0a), with higher concentrations over the center of mid-latitude gyres, a.k.a. garbage patches including the North Pacific, South Pacific, North Atlantic, South Atlantic, and Indian Ocean[30]. The coastal regions of Asia, Europe, and North and South America also experience higher DOC releases due to riverine and coastal plastic emissions[31–33]. The plastic-released DOC, largely treated the same as the plankton-derived DOC, affects the carbon biogeochemical cycle by both providing an extra carbon source for microbial respiration and increasing the existed organic carbon content of seawater, which may further influence the sea-to-air CO_2 exchange[19] (See Methods). We calculate the increase in oceanic CO_2 flux from the sea to the air caused by plastic-released DOC (0b). Our model reveals that plastic-released DOC weakens global oceanic CO_2 uptake by 0.0044 TgC yr^{-1} (0b). The increase in CO_2 flux due to released DOC largely overlaps with the spatial distribution of the DOC but is more concentrated in the mid- and low-latitude oceans. This reflects differences in seawater chemical factors such as pH value and the buffer capacity, as well as the metabolic activity of marine organisms primarily mediated by the temperature[7]. While the increased organic carbon from oceanic plastics could potentially contribute to ocean acidification as an added carbon source, the impact on ocean acidification is currently negligible at present plastic concentrations. Our modeling results suggest that the change of the concentration of hydrogen ions (H^+) due

to plastic-released DOC is less than 0.001% even in oceanic areas with high plastic abundance such as the North Pacific Garbage Patch (NPGP).

Toxicity effects on phytoplankton communities Ocean plastics could harm marine phytoplankton due to their toxicity effects, with further implications on the marine carbon cycle (0). We combine the marine ecosystem model with the oceanic plastic simulation by considering the plastic toxicity effect on the growth of phytoplankton (see Methods). In the ecosystem model, *Diatoms*, *Other large* (large fast-growing eukaryotes other than *Diatoms*)[7], *Synechococcus,* and *Prochlorococcus* with varying sizes, affinity to different nutrients, and growth rate, are selected as representative function groups of the marine phytoplankton communities due to their crucial roles in marine net primary production (MNPP) and oceanic CO_2 uptake[7,27]. The distributions of the biomass of these four marine phytoplankton groups without the influence of plastics are illustrated in 0a1-a4. *Diatoms*, with high affinity to silica, predominantly inhabit high-nutrient waters such as the middle and high-latitude regions of the Atlantic, Indian Ocean, and Pacific Ocean. In contrast, *Other large* are relatively more concentrated in the Arctic Ocean according to our simulation. *Synechococcus*, which shares similar habitat preferences with *Diatoms*, is more abundant along the northern coast of the Indian Ocean[34]. *Prochlorococcus*, with the smallest size, has a complementary distribution to *Diatoms* and *Synechococcus*. It is abundant in the open ocean between 40°N and 40°S due to being outcompeted by other phytoplankton in high-nutrient waters[34]. The vertical distribution of both oceanic plastics and marine phytoplankton are considered in our model as both of them are 3-D distributed in our model. We only discuss the overall growth change of phytoplankton within the top 100 m due to the concurrent presence of phytoplankton and plastics.

We find distinct spatial patterns for the toxicity effects of oceanic plastics, contingent on the plastic abundance and plankton community structures. We first assess changes in phytoplankton growth resulting from plastic toxicity and competition within the marine phytoplankton community in the Combined Toxicity Effect (Max) Scenario (0b1-b4), which considers the combined toxicity effects of all plastic types. This scenario is categorized into “Max”, “Middle”, and “Min” scenarios by selecting maximum, middle and minimum toxicity effect parameters, respectively, given their substantial variability in literature (see Methods). The results suggest that the phytoplankton growth is more severely impacted in plastic-abundant areas including the Pacific Garbage Patches, the western subtropical Pacific Ocean (particularly the coastal regions), the subtropical Atlantic Ocean, and the north Indian Ocean. Although all phytoplankton are affected in those plastic-abundant areas, those impacts are further intensified, mitigated, or even reversed due to community competition, as reflected in the growth change rate of the four phytoplankton functional groups (0b1-b4). For example, *Diatoms* and *Synechococcus* dominant in the Pacific Garbage Patch, exhibit contrasting responses due to community competition and toxicity effects from different plastics. The Pacific Garbage Patch can be divided into two areas (hereafter referred to as the west and east, 0b1-b4) based on the opposite distribution of plastic concentration and phytoplankton biomass. Phytoplankton is more abundant in the west while the concentration of plastics is considerably higher in the east due to PE and PP (Figure.

S8 and Figure. S11). The growth of *Synechococcus* in the west is inhibited by relatively high concentrations of PVC, PS, and ABS. This leads to increased NO_3 and PO_4 concentrations due to decreased absorption by *Synechococcus*. The favorable nutrient condition largely mitigates the negative effects of plastics on *Diatoms*, resulting in increased growth change rate and biomass (~12% as shown in 0b1). These growth changes also contribute to an increase in total biomass of the phytoplankton community. On the contrary, a much higher concentration of plastics in the east restricts the growth of both *Diatoms* and *Synechococcus*, particularly the former with a maximum decrease of -4%. The concentrations of NO_3 (0.44%) and PO_4 (0.10%) are slightly elevated in the west, promoting the growth of *Prochlorococcus*, but there remains a net decrease in the total biomass of the phytoplankton community.

Similar growth change patterns of phytoplankton impacted by oceanic plastics can also be found in other areas such as the east and southeast Asian coastal areas, the subtropical ocean areas, and the north Indian Ocean areas. The East Asian coastal area, characterized by high plastic abundance, is also the main habitat of *Diatoms*, *Synechococcus,* and *Prochlorococcus*. However, our modeling results suggest distinct changes in the growth pattern of these groups. *Diatoms* suffers from the impairments of multiple polymer types of oceanic plastics as their growth decreases by more than 1%. Conversely, the growth of *Synechococcus* and *Prochlorococcus* benefits from the loss of *Diatoms* there, offsetting the direct toxicity effect by plastics. Moreover, the model also suggests the adverse growth change patterns of *Other large* and *Synechococcus* in the southeast Asian coastal area, another oceanic-plastic-abundant sea area. This underscores the regulatory role of community competition in modulating the impact of plastics on different phytoplankton functional groups (0b1-b4). The growth changes of phytoplankton in the Indian Ocean also highlight the role of intergroup competition, with the growth of *Synechococcus* decreasing, while the growth of *Prochlorococcus* increasing. Indeed, all phytoplankton types are potential victims of this oceanic plastic intrusion, but the 'winner' and 'loser' vary across different areas based on specific biogeochemical characteristics while oceanic plastics are reshaping the phytoplankton community structure and the marine ecosystem.

The toxicity of plastic on phytoplankton may further impact the oceanic CO_2 flux as a result of the growth rate changes. We find a net increase in air-to-sea CO_2 flux of up to 0.82 TgC yr^{-1}, attributed to the toxicity effect of plastics on marine phytoplankton (the Combined Toxicity Effect (Max) scenario, 0b5). Increased CO_2 flux from the ocean to the atmosphere is simulated in the Indian Ocean, the Atlantic Ocean, and the Northwest Pacific Ocean, while the CO_2 intake flux (i.e., from the atmosphere to the ocean) is enhanced in the Northeast Pacific Ocean, southeast Asia, and the junction of the Atlantic and Arctic Oceans compared to the flux without plastic effects (0a5). The spatial distribution of oceanic CO_2 uptake changes generally aligns with the overall growth rate changes of different phytoplankton functional groups. Specifically, the varying impairments of oceanic plastics on phytoplankton result in differing impacts on photosynthesis, as indicated by changes in chlorophyll content across different regions. For example, the significant increase in *Diatom*-related (~7.2%) and *Prochlorococcus*-related (~0.3%) chlorophyll contents due to growth change in the

west and east Pacific Garbage Patch leads to distinct oceanic CO_2 uptake change as shown in 0b5. The modeled increase of CO_2 uptake in the Southeast Asian coastal area can also be explained by the enhanced photosynthesis of increased *Other large* (~1% increase of *Other large*-related chlorophyll). Similarly, the subtropical ocean areas exhibit significant CO2 flux changes due to the interplay of toxicity effects from abundant oceanic plastics and the high metabolic activity of phytoplankton in these areas.

Implications Our simulations are subject to considerable uncertainties. We establish multiple scenarios to bracket the range of these uncertainties and assess sensitivities of assumptions we make in our simulations, including the abundance of plastics in the ocean, the releasing rate and bioavailability of plastic-released DOC, and the dose-effect relationship for the toxicity effects of plastics (see Methods and the SI Text). Using different ocean plastic abundance can significantly affect the impacts of plastics on the marine carbon cycle through all three pathways mentioned above (e.g. -0.10 to 3.76 TgC yr^{-1} of oceanic CO_2 uptake change from toxicity effects). Varying the parameters for plastic DOC-releasing alters its impacts by a factor of ~4%, whereas different parameters for plastic toxicity have even greater effects on both phytoplankton community and oceanic CO_2 uptake (0.02 to 0.82 TgC yr^{-1}). Additionally, relative size effect can effectively mitigate the toxicity effects of plastic and their cascading effects (reducing the original impact by 96%). We also examine the interactive effects of these uncertainties, which could lead to a maximum reduction in oceanic CO_2 uptake by 12.08 TgC yr^{-1} (more detail in the SI Text). Despite these uncertainties, our model can still be interpreted as a diagnostic tool and hypothesis generator similar to the ModeEx approach (https://ess.science.energy.gov/modex/). It helps to reveal potential ways and modes of the interaction between oceanic plastic and the marine carbon cycle. Furthermore, the model results can also guide further experimental and field studies to fill knowledge gap and reduce model uncertainties.

Plastic is made of crude oil or natural gas, and recycled plastic products or plastics sequestered in landfills which are stable enough to hardly release CO_2 to the atmosphere in a decadal time scale. Thus, once buried, most plastic C can be assumed to be stable [38]. However, we find the impacts of plastics on the marine ecosystem and carbon cycle. In our simulation, oceanic plastics may reduce oceanic carbon uptake by 0.22 TgC yr^{-1} even in the Combined Toxicity Effect (Middle) scenario, which is 31% of oceanic plastic emission (0.70 (0.13-3.8) Tg yr^{-1}), and such impact also ranges from -0.10 to 12.08 TgC yr^{-1} for different scenarios (See Table S1). It is noteworthy that oceanic plastic pollution and these impacts are long-lasting due to the slow degradation rate of plastic in the oceanic environment. The cumulative extra sea-to-air CO_2 flux may reach 0.4 PgC by 2050 (ranged from -0.003 to 0.4 PgC), a time scale relevant to current climate policies and most of the released plastic can last even longer, if we assume the ocean plastic emissions remain steady at the present-day level. This value may be further expanded to approximately 1.6 PgC (at maximum), which is between the annual greenhouse gas emissions of the world's largest (3.0 PgC) and second-largest (1.2 PgC) emitting countries in 2020, as plastic production is increasing at a rate of 8.4% per year[29,35]. There are additional carbon emissions during processes like plastic production,

transport, and utilization, which also have considerable carbon footprint but are not included in this study[36]. Numerous laboratory studies have demonstrated the significant impacts of plastics on the marine carbon cycle such as 45% reduction in carbon export under relatively high plastic concentrations[10,37]. With the increase of plastic emission, the impacts of oceanic plastics are even more important in the future, contrasting with a likely decreasing or even fully neutralized CO_2 emissions from energy production and other industrial sectors[38]. Moreover, our results suggest that oceanic plastic debris may have complex impacts on the plankton community structure and primary production, which fuel the ocean ecosystem and have many cascading effects on oceanic CO_2 uptake, O_2 production, fisheries and aquaculture, marine food webs, and on vital ecological functions and ecosystem service of the ocean[34]. Oceanic plastic can also affect various trophic levels in marine ecosystems, including zooplankton[42]. These effects would further compound and amplify the impact of plastics on the marine carbon cycle, and our simulation is relatively conservative.

Oceanic plastic concentrations are generally higher in nearshore areas as it is close to emission sources such as estuaries and coastal cities. Phytoplankton and primary production are also abundant in these areas due to nutrient repletion and reduced predation, and CO_2 intakes are correspondingly high in these areas, constituting a significant blue carbon sink. Nearshore areas are thus potentially a hotspot for the impact of plastics on the ocean ecosystem and carbon cycle. While the resolution of our model is relatively coarse to directly model this impact, similar impact modes and influencing factors as the open ocean may still apply. Indeed, our current estimation of the impact of oceanic plastic is conservative, and we call for further research on this topic.

The varied chemical and physical properties of oceanic plastic polymers lead to difference in their cycle processes and spatial distributions in the ocean, which is also the basis for their varying impacts on the marine carbon cycle. Combined with their distinct toxicological and DOC-releasing characteristics[14,18,20–26,39,40], the differing stocks of these oceanic plastics contribute more unevenly to the impact on marine biogeochemistry and carbon cycling. The varied impacts of oceanic plastics are particularly reflected in the heterogeneity of their toxicity effects on different species of phytoplankton. Using PVC and PP as examples, PVC, with its higher density, tends to accumulate more on sediment and beaches than PP. However, PVC's lower carbon content reduces its contribution to the buried carbon (less than 40% of PP's contribution). Meanwhile, although the lower DOC-releasing capacity (PVC's $\boldsymbol{k_{DOC}}$ is about two orders of magnitude lower than PP) of PVC limits its impact on the marine carbon cycle through the DOC pathway, the significant ecological toxicity of PVC has resulted in a more noticeable impact on phytoplankton growth and sea-to-air CO_2 exchange compared to PP (Figure. S2). Other factors such as the toxicity effect model and parameters, the relative size effect, the plastic abundance effect, and the community competition could further exacerbate the complexity of the potential impacts of plastics on the marine carbon cycle. Higher or lower toxicity effect parameters or plastic abundance could significantly and nonlinearly strength or weaken plastics impacts on phytoplankton growth and ocean carbon uptake (Figure. S1-S4). The particle size can

also effectively alter the toxic effect of oceanic plastics on marine phytoplankton, with smaller size plastics generally exerting a greater toxicity effect (Figure. S3)[21,41]. Community competition may mitigate the damage of plastics to the growth of specific species of phytoplankton, or exacerbate the growth loss of other phytoplankton, depending on the phytoplankton's community structure and oceanic plastic concentration at different areas. Although the diversity properties of oceanic plastics and factors mentioned above complicates oceanic plastics effects on the ocean ecosystem and carbon cycle, these also encourages us to implement specific strategies for controlling marine plastic pollution to minimize oceanic plastics impact. Reducing oceanic plastic emissions could effectively reduce the impact on marine ecosystem and ocean carbon uptake. Existing oceanic plastics should be controlled as early as possible before they are washed and worn into smaller microplastics, or even nanoplastics, to prevent their damage to the marine microbial community as well as the marine carbon cycle. Plastic types with higher phytoplankton toxicity and ocean carbon footprint (such as PVC and PS) should be controlled with higher priority. The cleaning up of oceanic plastics in phytoplankton colonies that have significant implications for ocean carbon uptake should be given top priority. Overall, we emphasize the need to consider the impact of plastic debris on ocean biogeochemical and carbon cycle when formulating plastic and climate change policies, such as the ongoing and future negotiation for the global plastic treaty (Intergovernmental Negotiating Committee on Plastic Pollution)[42]. We suggest that delaying action on plastic pollution may undermine our endeavors to combat climate change, impede our progress towards sustainable development, and compromise the functioning of ecosystems and their associated services. Immediate actions are necessary to mitigate plastic pollution and alleviate its impacts on the carbon cycle and climate change.

Methods

Oceanic plastic simulation We simulate the transport and transformation of oceanic plastic with different chemical compositions and sizes in the Nanjing University Marine Plastic Model (NJU-MP). This model is based on the model framework of MITgcm (Massachusetts Institute of Technology General Circulation Model)[43]. The resolution of NJU-MP is 2° × 2.5° horizontally as well as 22 levels vertically, and its time step is 4 h. Five polymer type of oceanic plastics with different densities are included in this model: PE, PP, PVC, PS, and ABS, and each of them has six diameter groups: <0.0781, 0.0781–0.3125, 0.3125–1.25, 1.25–5, 5–50 and >50 mm. The model depicts the processes by which plastic waste enters and circulates within the ocean, including sinking and rising, drifting, fragmentation/abrasion, beaching, and biofouling and defouling. These processes depend on intrinsic properties of plastic such as density, as well as exterior influences of circulation, marine plankton, etc. The model is run from 1950 to 2020, and the simulated distribution and fluxes of plastic by the end of 2020 are used to further model the plastics' impacts on marine ecosystem as well as marine carbon cycle.

Three plastic emission sources: the riverine plastic emission, the coastal plastic emission, and the ocean plastic emission are used in our oceanic plastic simulation. The

riverine plastic emissions are plastic debris carried by river water, so their spatial pattern follow as the locations of estuaries from major rivers worldwide[32]. The coastal plastic emissions are closely related to coastal areas, primarily from coastal residents[33]. Both riverine and coastal emissions derive from terrestrial environment, influenced by factors such as plastic consumption, waste management and population density. Direct ocean plastic emissions refer to plastics discharged from fisheries and shipping, and its spatial pattern is consistent with the global footprint of fisheries and shipping tracks[44,45]. In this simulation, cumulative plastic production is used as a proxy for historical trend of plastic emissions, with polymer types allocated based on global consumption data in 2013[29]. Discharged plastics are initially divided into micro-plastics (<5 mm) and macro-plastics (>5 mm) in emission sources, then the diameters groups are expanded to six after fragmentation and abrasion processes of our model.

The sinking and rising of oceanic plastics in our model are determined by their densities, diameters, shapes, and the state of seawater. The drifting process, also known as leeway drift or windage, is affected by five forces including gravity, buoyancy, seawater stress, horizontal wind stress and Coriolis force. The fragmentation/abrasion rate varies with the polymer type and shape of oceanic plastics, and depends on environmental factors such as sunlight. In our simulation, beaches bi-directionally exchange plastics with the ocean. Based on the length of sandy beaches within a model grid, we set an effective beaching rate between 0.15% to 1.1% day^{-1}, with part of beached plastics accumulating over time. In our model, biofouling and defouling are represented as the attachment and release of oceanic plastics with biomass including microbes, phytoplankton, zooplankton, and marine snow based on Kooi et al.[3].Those processes can change densities of oceanic plastics, and further affect the vertical and horizontal transport of oceanic plastics in the sinking, rising and drifting process in our modeling. More details of each process can be found in Zhang et al.[1].

Model ensemble and optimal estimation There are multiple sources of uncertainty for the plastic emissions simulated by NJU-MP model. The model parameters and process settings, as well as the oceanic plastic emission sources setting are the main sources of uncertainness. The former includes the value of different parameters in different processes such as the different fragmentation rate (3% to 30% per year) and varied biofouling rate (based on the biomass data of plankton) for different plastic polymer types[1]. The latter originates from different emission inventories[34,35,50]. To assess these uncertainties, a model ensemble is constructed by randomly generating model parameters[1]. This ensemble consists of 156 modeling scenarios driven by varying model parameters (generated by using a Monte Carlo approach) such as fragmentation, biofouling, sedimentation, beaching rates, as well as emission inventories. These model members are further optimized by constraining them with observation data of ocean surface plastic through a super ensemble three-dimensional variational method[91]. The optimized model performs well in capture the trend of the vertical profile of oceanic plastics[1]. The optimal estimates of plastic discharged to the global ocean from these model scenarios range from 0.13–3.8 million Mt (metric tons) yr^{-1}, spanning approximately 1.5 orders of magnitudes. We select three scenarios representing min (0.13 million Mt yr^{-1}), middle (0.70 million Mt yr^{-1}), and max (3.8

million Mt yr^{-1}) estimates of oceanic plastic emission as the min, the middle, and the max plastic abundance for further modeling of plastic impacts on marine carbon cycle[1].

Marine ecosystem model We use the Darwin ecosystem model to simulate the impact of plastics on the marine carbon cycle by coupling with the plastic model[7,27]. The coupled model has the same spatial resolution and time step as the NJU-MP model. The Darwin ecosystem model has been widely used in examining the interplay between marine ecosystem and biogeochemical cycles[7,46]. Six phytoplankton functional groups (*Diatom*, Other large, *Prochlorococcus, Synechococcus, Coccolithophore, and Diazotrophs*) and two zooplankton (small and large) functional groups are included to represent the marine plankton community. The biogeochemical cycles of inorganic and organic forms of carbon, nitrogen, phosphate, phosphorus, iron, and silica are simulated through the interaction with marine ecosystems. This model also includes the feed, graze, and mortality process of marine plankton, as well as the transformation of elements such as the air-sea CO_2 exchange process. We select *Diatoms*, Other large, *Synechococcus,* and *Prochlorococcus* to study the impacts of plastics on the marine ecosystem and carbon cycle. This simulation spans from 2000 to 2020, and we use the results of 2020 as the baseline for further analysis. The Darwin ecosystem model is used simulate the specific impacts of oceanic plastics on the ocean carbon cycle including the process and magnitudes, and the structure of coupled model is shown schematically in **Error! Reference source not found.**.

The diversity and biogeography of plankton communities are key for modeling plankton communities. The Darwin ecosystem model explores numerous characteristics such as cell size and nutrient affinity, as well as functions traits such as ingestion and growth of phytoplankton to understand them. The Darwin ecosystem model can simulate more complex functions and relationships such as the community competition and top-down control based on basic characteristics and function traits. We simulate oceanic plastics' impacts on marine phytoplankton communities to understand how plastics impact marine ecosystem. Specifically, we select *Diatoms*, *Other large*, *Synechococcus,* and *Prochlorococcus* to investigate the toxicity effect of plastics on the growth of marine phytoplankton community as these four are the major contributors to the total ocean primary productivity and phytoplankton biomass[34,46].

The elemental cycle in the Darwin ecosystem model are jointly determined by both biogeochemical transformation and biological activities. For example, inorganic nutrients in surface ocean can finally be transformed as sinking particulates in the sea bed through ingestion, mortality, grazing, egestion of plankton, and formation, transformation and remineralization process. We focus on the response of marine carbon cycle to the marine ecosystem change under the impacts of oceanic plastics. Meanwhile, we also treat DOC-releasing of plastics as another way of plastics impacting marine carbon cycle by adding plastic-released DOC into oceanic DOC cycle as an extra DOC sources in the coupled model. These impacts on marine carbon cycle are further examined by the change of oceanic CO_2 uptake.

Buried Carbon Oceanic plastics buried in the ocean sediments are hardly involved in marine biochemical reactions[6], so we treat them as the increase of buried carbon. Such

buried carbon comes from both plastics' direct sinking and indirect sinking resulting from biofouling which can alter plastic's density. Beached plastics serve as a transfer reservoir of oceanic plastics with part of beached plastics remains and accumulates there. Thus, we also treat beached plastics as a net increase of buried carbon. Based on the simulation results of sedimented plastics and beached plastics, we calculate buried carbon from these two sources by multiplying the carbon content of each polymer type of oceanic plastics:

$$C_{sediment} = \sum\sum P_{ij} A_j C_i \quad (1)$$

where $C_{sediment}$ denotes the mass of buried carbon from sedimented and beached plastics every year (TgC yr^{-1}). P_{ij} is the concentration of polymer type i of oceanic plastic in grid j (#m^{-2}), and A_j is the area of grid j. C_i denotes the percentage of carbon content for five polymer types of oceanic plastics we calculate based on their chemical structures.

DOC releasing Under light irradiation, oceanic plastics can leach DOC at a certain rate depending on the polymer type of plastics. Plastic related DOC leaching conforms to zero-order or first-order reaction kinetics[14,39,40]. To simplify this process, we choose a fixed leaching rate for different polymer types as depicted in Table S5. Such release rate drops to a minimum value in the dark environment[14,39,40]. We treat the rate constant of reaction of plastic-DOC-leaching as the DOC releasing rate, and calculate the released DOC based on the seawater plastic concentrations and their DOC releasing rate:

$$P_{DOC} = P_{ij} k_{DOCi} \exp(-atten_j) Bio_i \quad (2)$$

where P_{DOC} is the concentration of DOC leached from polymer type i of oceanic plastics in grid j with same units as DOC (mmol·m^{-3}). k_{DOCi} denotes the DOC releasing rate constant of different oceanic plastics, and this equation is also modified by $atten_j$ which is the light irradiation attenuation of each grid attenuated by depth, chlorophyll, planktons, and dissolved and particulate material[47]. We first convert DOC-releasing rate from laboratory studies to a rate of uniform light intensity based on their experimental conditions, and use the average value of these rates as DOC releasing rate for each polymer types of plastics under fully illuminated conditions. Then we use the same light attenuation coefficient ($atten_j$) to represent the % of DOC-releasing rate decrease with ocean depth. As few studies measure the DOC releasing rate of ABS, we use the average value of the DOC releasing rate of PVC and PS, both amorphous plastics, to represent ABS's DOC releasing rate based on their similar chemical and physical properties. We adapt high, middle, and low data set of k_{DOCi} based on laboratory studies as shown in Table. S5. Our modeled mean value of total plastic-released DOC is only 0.25 TgC yr^{-1}, which is only nearly 0.0012% biogenic DOC production rate and 0.0005% of total DOC pool in our model[48]. Thus, we assume plastic-released DOC has the same conversion process as the plankton-derived DOC in our model. Plastic-released DOC in our model can increase the plankton-derived DOC pool and can be utilized by microbes, ultimately being converted to dissolved inorganic carbon (DIC) and CO_2

through biological processes within the ocean carbon cycle. Based on the proportion of bioavailable plastic-released DOC[17,43,44], we also modify this equation with the bioavailable fraction Bio_i. We use the average value of percentage of bioavailability from laboratory studies as shown in Table S9. Plastic-released DOC may disturb the marine carbon cycle in both ways, and further affect the air-to-sea CO_2 exchange. Therefore, we use the change of oceanic CO_2 uptake as an indicator to evaluate the overall impacts.

Growth change of phytoplankton The detrimental effects of most oceanic plastics on phytoplankton's cell morphology and photosynthesis may ultimately impact their growth, and several laboratory studies have investigated the response of phytoplankton growth rates to plastic concentrations[17–26,41,49–53] These impacts suggested by laboratory studies are significant as the concentration of added plastic debris in these studies are relatively high. To investigate the toxicity effect of oceanic plastics, we derive the growth impact parameters from the growth curve or growth data (the former is based on the latter) of phytoplankton under different concentration of plastics from several studies[17–25,41,49–53]. Details about growth impacts parameters can be found in Table S6, S7 and S8. We calculate the growth rate of phytoplankton as a function of plastic concentrations:

$$GrowthP_{ijs} = GrowthI_{js} \exp(-Param_{is} P_{ij}) \quad (3)$$

where $GrowthP_{ijs}$ denotes the growth of species s of phytoplankton in grid j under the exposure of polymer type i of plastics. $GrowthI_{js}$ is the original growth rate of species s of phytoplankton in grid j without plastics[7,27]. $Param_{is}$ is the toxicity effect parameter of polymer type i of oceanic plastics on species s of phytoplankton derived from laboratory studies which are not complete for all plastics and all phytoplankton, so we use same $Param_{is}$ of PS to represent $Param_{is}$ of ABS for all phytoplankton; use $Param_{is}$ of PE to represent $Param_{is}$ of PP for the growth impacts on *Synechococcus* and *Prochlorococcus*; use $Param_{is}$ of PVC to represent $Param_{is}$ of PS for the growth impacts on *Prochlorococcus*. The value of $Param_{is}$ not only depends on the polymer type of plastics and the species of phytoplankton but also varies even for the same plastics and the same phytoplankton due to different experimental subjects and methods chosen in those laboratory studies[17–25,41,49–53]. We follow this equation to consider the effect of each individual plastic polymer type (the Independent Toxicity Effect Scenario). We also investigate the combined toxicity effects of all oceanic plastics on each phytoplankton by multiplying their growth impacts as different polymer types of plastics are dispersed around phytoplankton:

$$GrowthP_{js} = GrowthI_{js} \prod \exp(-Param_{is} P_{ij}) \quad (4)$$

where $GrowthP_{js}$ denotes the growth of species s of phytoplankton in grid j under the exposure of all oceanic plastics. Due to differences in experimental conditions, different studies may have different results on the toxicity effects of the same polymer type of oceanic plastics on the same phytoplankton species. We select the maximum, middle

and minimum parameters to investigate how dose-effect affect the growth impacts of oceanic plastics:

$$GrowthPtoxic_{js} = GrowthI_{js} \prod \exp(-Paramtoxic_{is} P_{ij}) \quad (5)$$

where $GrowthPtoxic_{js}$ is the growth of species s of phytoplankton in grid j under the exposure of all oceanic plastics with max, middle, or min toxicity effect parameters. $Paramtoxic_{is}$ denotes the max, middle, or min toxicity effect parameters of polymer type i of oceanic plastics on species s of phytoplankton for each phytoplankton. We also include the relative size effect by multiplying the relative size effect parameters:

$$GrowthPsize_{js} = GrowthI_{js} \prod \exp(-Param_{is} P_{ij} Paramsize_{isg}) \quad (6)$$

where $GrowthPsize_{js}$ is the growth of species s of phytoplankton in grid j under the exposure of all oceanic plastics which is modified by the relative size effect. $Paramsize_{isg}$ denotes the relative size effect parameter for each phytoplankton and g denotes the relative size groups. We divide the $Paramsize_{isg}$ into different groups based on both the diameter of different oceanic plastics and the size of phytoplankton. Specifically, there are three groups for *Diatoms*: <0.3125, 0.3125—5 mm, >5 mm; three groups for *Other large*: <0.0781, 0.0781–1.25, >1.25 mm; two groups for *Prochlorococcus* and *Synechococcus*: <0.0781, >0.0781 mm (See Table S2). Plastic abundance can also affect the growth impacts of oceanic plastics on phytoplankton via higher or lower concentration of oceanic plastics. We include the plastic abundance effect based on different plastic simulation scenarios:

$$GrowthPplastic_{js} = GrowthI_{js} \prod \exp(-Param_{is} P_{ijp}) \quad (7)$$

where $GrowthPplastic_{js}$ is the growth of species s of phytoplankton in grid j under the exposure of different concentration of oceanic plastics. P_{ijp} is the concentration of polymer type i of oceanic plastic in grid j (#m^{-2}) in plastic simulation scenario p.

Scenario settings We design various scenarios to comprehend the influence of factors such as plastic toxicity parameter settings, uncertainties related to plastic abundance, and the role of relative size effects in the process of plastic impacting the marine carbon cycle (Table S1). We use the middle plastic abundance as the baseline of oceanic plastic emission to investigate the mean value of plastic-related buried carbon and the impacts plastic-released DOC (middle DOC releasing rate is also used) as shown in 0 and 0. We also estimate the upper and lower bound of buried carbon by adapting the max and min plastic abundance as shown in Table S2. The upper and lower bound of impacts of plastic-released DOC on marine carbon cycle are estimated by using max and min plastic abundance as well as high and low DOC releasing rate as shown in Table S3. Based on the middle plastic abundance, we combine toxicity effects of each plastic on all phytoplankton species as the Combined Toxicity Effect scenario, and we select different toxicity effect parameter (Max (0b1-b5) Min and Middle (Figure. S1a1-a4 and

Figure. S1b1-b4)) for evaluating uncertainties; we design the Independent Toxicity Effect scenario to investigate how oceanic plastic with single polymer type (PE, PP, PVC, PS, and ABS) impacts marine phytoplankton individually (Figure. S2a1-a5); we consider the relative size effect of plastic-phytoplankton pairs by setting different relative size pair groups as the Relative Size Effect Scenario (Figure. S3a1-a5 and see Table S4 for more details). Then, we combine the middle toxicity effect parameters with max and min oceanic plastic emission as Plastic Abundance (Max) Scenario (Figure. S5a1-a5) and Plastic Abundance (Min) Scenario (Figure. S4b1-b5). We also investigate the joint impacts of max toxicity effects and max plastic abundance by combining toxicity effect parameters from the Combined Toxicity Effect (Max) and oceanic plastic emission of Plastic Abundance (Max) scenario as the Combined Toxicity Effect (Max) & Plastic Abundance (Max) Scenario (Figure. S5a1-a5). Plastic-released DOC may also contribute to air-to-sea CO2 flux change in these toxicity-related scenarios as it can be utilized by microbes as nutrients. However, we consider the interactions with nutrient demand by phytoplankton is rather small as carbon is not a typical limiting nutrient for phytoplankton growth. In addition, plastic-released-DOC is also much smaller than the existing plankton-derived. Thus, we only present results of one scenario which incorporate the impact of plastic-released DOC into the impact of plastics toxicity effect on the oceanic CO_2 uptake change simultaneously as the Combined Toxicity Effect (Include DOC) scenario (See Table S1).

Model sensitivity We test the sensitivity of model results of air-to-sea CO_2 flux change to key model parameters as depicted in Table S9 and Figure. S7. Sensitivity of plastic DOC releasing is tested by using different DOC releasing rates, plastic abundance as well as considering bioavailable scenario as shown in Figure. S7a. We also teste sensitivity of plastic toxicity effects to plastic abundance, toxicity effect parameter, size effect and DOC-releasing effect (Figure. S7b).

Data availability

All data are available in the article, the supplementary materials, or the website: https://zenodo.org/records/16722412.[57] Materials & Correspondence should be addressed to Yanxu Zhang.

Code availability

All model code is available at the website: https://zenodo.org/records/16722412.[57]

Acknowledgments We appreciate Dr. Amina T. Schartup and Dr. Emily Zakem for the helpful discussions and suggestions. This study is supported by the Postgraduate Research & Practice Innovation Program of Jiangsu Province (KYCX23_0125) (to Q.P.). Luisa Galgani was supported by the Italian Ministry of University and Research funded by the European Union-Next Generation EU, project code CN_00000033, CUP B63 C22000650007, project title “National Biodiversity Future Center-NBFC” (to L.G.).

Author contributions Statement Conceptualization: Y.Z., Q.P.; Methodology: Q.P., P.W., X.W., Z.Z., T.Y.; Investigation: Q.P., P.W.; Visualization: Q.P., P.W., X.W.; Funding acquisition: Q.P.; Project administration: Y.Z.; Supervision: Y.Z.; Writing—

original draft: Q.P., Y.Z.; Writing—review & editing: Y.Z., Q.P., L.G., T.Y. H.W.

Competition interests Statement

The authors declare no competing interests.

Figure Legends

Figure. 1 | Schematic of coupled model in this study

Figure. 2 | Plastic carbon buried in sediments and beaches. a,b Modeled spatial distribution of buried carbon from sedimented plastics and beached plastics. c Proportion and mass of different polymer types of plastics and their contributions to buried carbon. d Vertical cumulative mass of sedimented plastic with different depths under the sea surface (We chose carbon storage in 2020 as the baseline of current annual buried carbon from oceanic plastics)

Figure. 3 | Impacts of DOC released by marine plastic on the ocean carbon cycle. **a** Sea surface DOC change, and **b** Sea to air CO_2 flux change

Figure. 4 | Toxicity effect of oceanic plastic on phytoplankton biomass/growth over the top 100m depth and sea-to-air CO_2 flux. a1-a4 Spatial distribution of marine plankton biomass without plastics. Phytoplankton growth change in the **b1-b4** Combined Toxicity Effect scenario (Max) (Red and blue box denote the west and east of the Pacific Garbage Patch, respectively). **a5** Spatial distribution of the mean annual sea-to-air CO_2 flux and **b5** sea-to-air CO_2 flux change in the Combined Toxicity Effect scenario (Max)

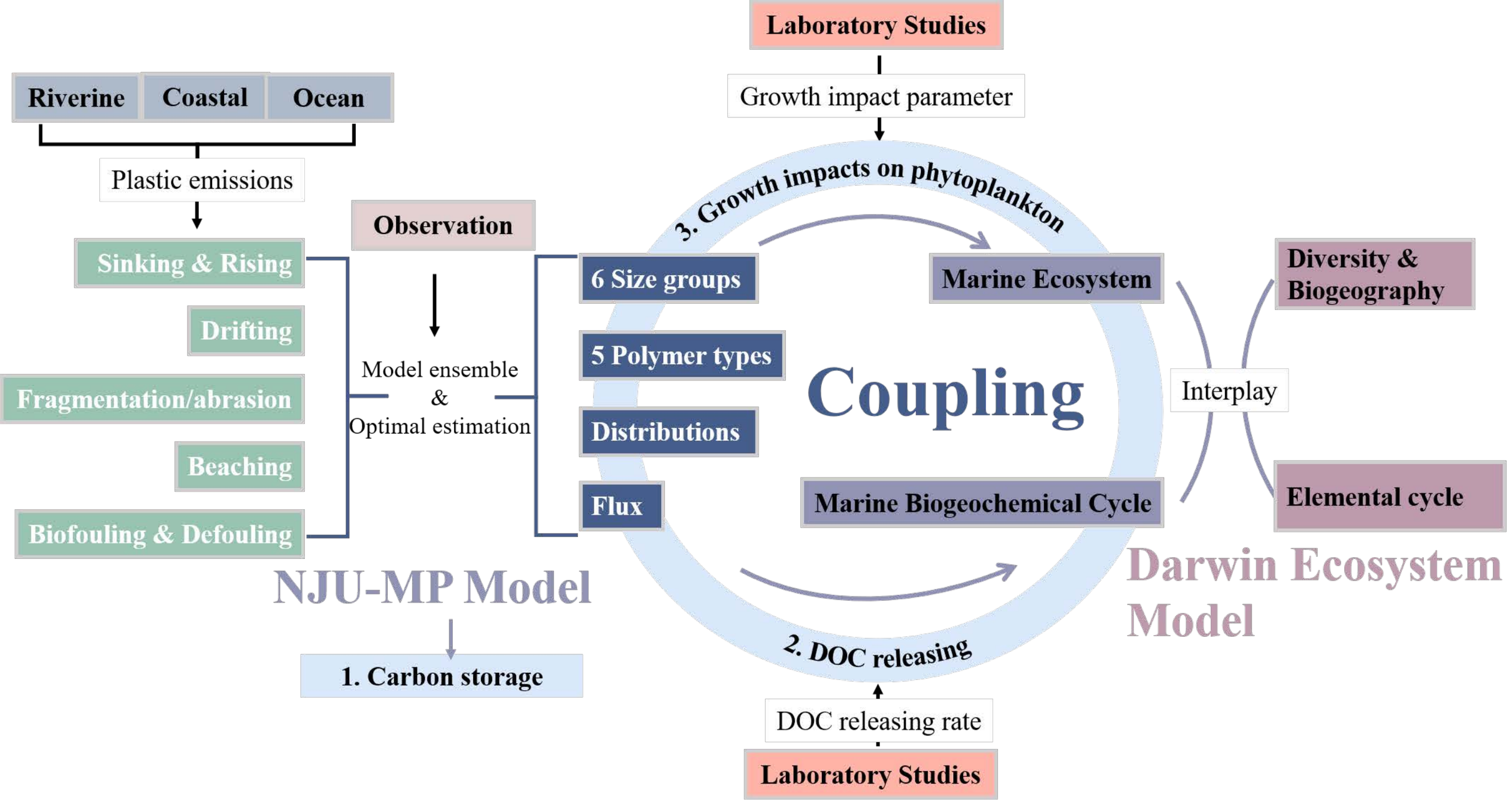
Reference

1. Zhang, Y. *et al.* Plastic waste discharge to the global ocean constrained by seawater observations. *Nat. Commun.* **14**, 1372 (2023).
2. Fu, Y. *et al.* Modeling atmospheric microplastic cycle by GEOS-Chem: An optimized estimation by a global dataset suggests likely 50 times lower ocean emissions. *One Earth* **6**, 705–714 (2023).
3. Kooi, M., Nes, E. H. V., Scheffer, M. & Koelmans, A. A. Ups and Downs in the Ocean: Effects of Biofouling on Vertical Transport of Microplastics. *Environ. Sci. Technol.* **51**, 7963–7971 (2017).
4. Allen, S. *et al.* Evidence of free tropospheric and long-range transport of microplastic at Pic du Midi Observatory. *Nat. Commun.* **12**, 7242 (2021).
5. Cressey, D. SCIENTISTS KNOW THAT THERE IS A COLOSSAL AMOUNT OF PLASTIC IN THE OCEANS. BUT THEY DON'T KNOW WHERE IT ALL IS, WHAT IT LOOKS LIKE OR WHAT DAMAGE IT DOES.
6. Galgani, L. & Loiselle, S. A. Plastic pollution impacts on marine carbon biogeochemistry. *Environ. Pollut.* **268**, 115598 (2021).
7. Dutkiewicz, S., Follows, M. J. & Bragg, J. G. Modeling the coupling of ocean ecology and biogeochemistry. *Glob. Biogeochem. Cycles* **23**, 2008GB003405 (2009).
8. Moran, M. A. *et al.* Deciphering ocean carbon in a changing world. *Proc. Natl. Acad. Sci.* **113**, 3143–3151 (2016).
9. Galgani, L. *et al.* Hitchhiking into the Deep: How Microplastic Particles are Exported through the Biological Carbon Pump in the North Atlantic Ocean. *Environ. Sci. Technol.* **56**, 15638–15649 (2022).
10. Roberts, C. *et al.* Microplastics may reduce the efficiency of the biological carbon pump by decreasing the settling velocity and carbon content of marine snow. *Limnol. Oceanogr.* **69**, 1918–1928 (2024).
11. Wu, N., Grieve, S. W. D., Manning, A. J. & Spencer, K. L. Flocs as vectors for microplastics in the aquatic environment. *Nat. Water* **2**, 1082–1090 (2024).
12. Intergovernmental Panel On Climate Change (Ipcc). *Climate Change 2021 – The Physical Science Basis: Working Group I Contribution to the Sixth Assessment Report of the Intergovernmental Panel on Climate Change*. (Cambridge University Press, 2023). doi:10.1017/9781009157896.
13. Regnier, P. *et al.* Anthropogenic perturbation of the carbon fluxes from land to ocean. *Nat. Geosci.* **6**, 597–607 (2013).
14. Alongi, D. M. *Blue Carbon*. (Springer International Publishing, Cham, 2018). doi:10.1007/978-3-319-91698-9.
15. Smeaton, C. Augmentation of global marine sedimentary carbon storage in the age of plastic. *Limnol. Oceanogr. Lett.* **6**, 113–118 (2021).
16. Romera-Castillo, C., Pinto, M., Langer, T. M., Álvarez-Salgado, X. A. & Herndl, G. J. Dissolved organic carbon leaching from plastics stimulates microbial activity in the ocean. *Nat. Commun.* **9**, 1430 (2018).
17. Kvale, K., Hunt, C., James, A. & Koeve, W. Regionally disparate ecological responses to microplastic slowing of faecal pellets yields coherent carbon cycle response. *Front. Mar. Sci.* **10**, 1111838 (2023).
18. Galgani, L. *et al.* Marine plastics alter the organic matter composition of the air-sea boundary

703 layer, with influences on CO2 exchange: a large-scale analysis method to explore future ocean
704 scenarios. *Sci. Total Environ.* **857**, 159624 (2023).
705 19. Sendra, M., Rodriguez-Romero, A., Yeste, M. P., Blasco, J. & Tovar-Sánchez, A. Products
706 released from surgical face masks can provoke cytotoxicity in the marine diatom Phaeodactylum
707 tricornutum. *Sci. Total Environ.* **841**, 156611 (2022).
708 20. Zhu, Z. *et al.* Joint toxicity of microplastics with triclosan to marine microalgae Skeletonema
709 costatum. *Environ. Pollut.* **246**, 509–517 (2019).
710 21. Zhao, T. *et al.* Microplastic-induced apoptosis and metabolism responses in marine
711 Dinoflagellate, Karenia mikimotoi. *Sci. Total Environ.* **804**, 150252 (2022).
712 22. Tetu, S. G. *et al.* Plastic leachates impair growth and oxygen production in Prochlorococcus,
713 the ocean's most abundant photosynthetic bacteria. *Commun. Biol.* **2**, 184 (2019).
714 23. Ge, J. *et al.* Microplastics impacts in seven flagellate microalgae: Role of size and cell wall.
715 *Environ. Res.* **206**, 112598 (2022).
716 24. Chae, Y., Kim, D. & An, Y.-J. Effects of micro-sized polyethylene spheres on the marine
717 microalga Dunaliella salina: Focusing on the algal cell to plastic particle size ratio. *Aquat. Toxicol.*
718 **216**, 105296 (2019).
719 25. Lagarde, F. *et al.* Microplastic interactions with freshwater microalgae: Hetero-aggregation and
720 changes in plastic density appear strongly dependent on polymer type. *Environ. Pollut.* **215**, 331–
721 339 (2016).
722 26. Galgani, L. *et al.* Microplastics increase the marine production of particulate forms of organic
723 matter. *Environ. Res. Lett.* **14**, 124085 (2019).
724 27. Feng, L.-J. *et al.* Short-term exposure to positively charged polystyrene nanoparticles causes
725 oxidative stress and membrane destruction in cyanobacteria. *Environ. Sci. Nano* **6**, 3072–3079
726 (2019).
727 28. Machado, M. C., Vimbela, G. V., Silva-Oliveira, T. T., Bose, A. & Tripathi, A. The response of
728 Synechococcus sp. PCC 7002 to micro-/nano polyethylene particles - Investigation of a key
729 anthropogenic stressor. *PLOS ONE* **15**, e0232745 (2020).
730 29. Follows, M. J., Dutkiewicz, S., Grant, S. & Chisholm, S. W. Emergent Biogeography of
731 Microbial Communities in a Model Ocean. *Science* **315**, 1843–1846 (2007).
732 30. Athanasiou, P. *et al.* Global distribution of nearshore slopes with implications for coastal retreat.
733 (2019).
734 31. Geyer, R., Jambeck, J. R. & Law, K. L. Production, use, and fate of all plastics ever made. *Sci.*
735 *Adv.* **3**, e1700782 (2017).
736 32. Lebreton, L. The status and fate of oceanic garbage patches. *Nat. Rev. Earth Environ.* **3**, 730–
737 732 (2022).
738 33. Mai, L. *et al.* Global Riverine Plastic Outflows. *Environ. Sci. Technol.* **54**, 10049–10056 (2020).
739 34. Lebreton, L. C. M. *et al.* River plastic emissions to the world's oceans. *Nat. Commun.* **8**, 15611
740 (2017).
741 35. Jambeck, J. R. *et al.* Plastic waste inputs from land into the ocean. *Science* **347**, 768–771 (2015).
742 36. Flombaum, P. *et al.* Present and future global distributions of the marine Cyanobacteria
743 *Prochlorococcus* and *Synechococcus*. *Proc. Natl. Acad. Sci.* **110**, 9824–9829 (2013).
744 37. World Bank Group. CO2 emissions (kt). *World Bank Open Data* https://data.worldbank.org
745 (2023).
746 38. Zheng, J. & Suh, S. Strategies to reduce the global carbon footprint of plastics. *Nat. Clim.*

Change **9**, 374–378 (2019).
39. Ziervogel, K. *et al.* Microbial interactions with microplastics: Insights into the plastic carbon cycle in the ocean. *Mar. Chem.* **262**, 104395 (2024).
40. DeAngelo, J. *et al.* Energy systems in scenarios at net-zero CO2 emissions. *Nat. Commun.* **12**, 6096 (2021).
41. Kvale, K., Prowe, A. E. F., Chien, C.-T., Landolfi, A. & Oschlies, A. Zooplankton grazing of microplastic can accelerate global loss of ocean oxygen. *Nat. Commun.* **12**, 2358 (2021).
42. Zhu, L., Zhao, S., Bittar, T. B., Stubbins, A. & Li, D. Photochemical dissolution of buoyant microplastics to dissolved organic carbon: Rates and microbial impacts. *J. Hazard. Mater.* **383**, 121065 (2020).
43. Lee, Y. K., Murphy, K. R. & Hur, J. Fluorescence Signatures of Dissolved Organic Matter Leached from Microplastics: Polymers and Additives. *Environ. Sci. Technol.* **54**, 11905–11914 (2020).
44. Zhao, T., Tan, L., Huang, W. & Wang, J. The interactions between micro polyvinyl chloride (mPVC) and marine dinoflagellate Karenia mikimotoi: The inhibition of growth, chlorophyll and photosynthetic efficiency. *Environ. Pollut.* **247**, 883–889 (2019).
45. United Nations Environment Programme. Intergovernmental Negotiating Committee on Plastic Pollution | UNEP - UN Environment Programme. https://www.unep.org/inc-plastic-pollution.
46. Marshall, J., Adcroft, A., Hill, C., Perelman, L. & Heisey, C. A finite-volume, incompressible Navier Stokes model for studies of the ocean on parallel computers. *J. Geophys. Res. Oceans* **102**, 5753–5766 (1997).
47. Kroodsma, D. A. *et al.* Tracking the global footprint of fisheries. *Science* **359**, 904–908 (2018).
48. Wang, X. *et al.* Ship emissions around China under gradually promoted control policies from 2016 to 2019. *Atmospheric Chem. Phys.* **21**, 13835–13853 (2021).
49. Weiss, L. *et al.* The missing ocean plastic sink: Gone with the rivers. *Science* **373**, 107–111 (2021).
50. Tréguer, P. *et al.* Influence of diatom diversity on the ocean biological carbon pump. *Nat. Geosci.* **11**, 27–37 (2018).
51. Smith, W. O. The relative importance of chlorophyll, dissolved and particulate material, and seawater to the vertical extinction of light. *Estuar. Coast. Shelf Sci.* **15**, 459–465 (1982).
52. Su, Y. *et al.* Microplastic exposure represses the growth of endosymbiotic dinoflagellate Cladocopium goreaui in culture through affecting its apoptosis and metabolism. *Chemosphere* **244**, 125485 (2020).
53. Ripken, C., Khalturin, K. & Shoguchi, E. Response of Coral Reef Dinoflagellates to Nanoplastics under Experimental Conditions Suggests Downregulation of Cellular Metabolism. *Microorganisms* **8**, 1759 (2020).
54. Liu, G., Jiang, R., You, J., Muir, D. C. G. & Zeng, E. Y. Microplastic Impacts on Microalgae Growth: Effects of Size and Humic Acid. *Environ. Sci. Technol.* **54**, 1782–1789 (2020).
55. Zhang, C., Chen, X., Wang, J. & Tan, L. Toxic effects of microplastic on marine microalgae Skeletonema costatum: Interactions between microplastic and algae. *Environ. Pollut.* **220**, 1282–1288 (2017).
56. Focardi, A. *et al.* Plastic leachates impair picophytoplankton and dramatically reshape the marine microbiome. *Microbiome* **10**, 179 (2022).
57. PANG, Q. Code and Data for The Potential Impacts of Plastic on the Marine Carbon Cycle.

Zenodo https://doi.org/10.5281/ZENODO.16722411 (2025).


Laboratory Studies
Growth impact parameter
Riverine
Coastal
Ocean
Plastic emissions
Observation
Sinking & Rising
Drifting
Fragmentation/abrasion
Beaching
Biofouling & Defouling
Model ensemble
&
Optimal estimation
6 Size groups
5 Polymer types
Distributions
Flux
3. Growth impacts on phytoplankton
Marine Ecosystem
Coupling
Marine Biogeochemical Cycle
2. DOC releasing
Interplay
Diversity &
Biogeography
Elemental cycle
NJU-MP Model
1. Carbon storage
Darwin Ecosystem
Model
DOC releasing rate
Laboratory Studies

Buried Carbon from Sedimented Plastic 0.13 TgC ·yr^{-1}

Buried Carbon from Beached Plastic 0.21 TgC ·yr^{-1}

a

b

10^{-1} 10^{0} 10^{1} 10^{2} 10^{3} 10^{4} 10^{5} g/km^2

c

Buried Carbon from Beached Plastic

Buried Carbon from Sedimented Plastic

Sedimented Plastic

Beached Plastic

Proportion In %

40 30 20 10 0 10 20 30 40

ABS PS PVC PP PE

0.4 0.2 0 0.2 0.4

Mass (Tg)

Total

d

Cumulative Sediment Plastic Mass

Total

PE

PP

PVC

PS

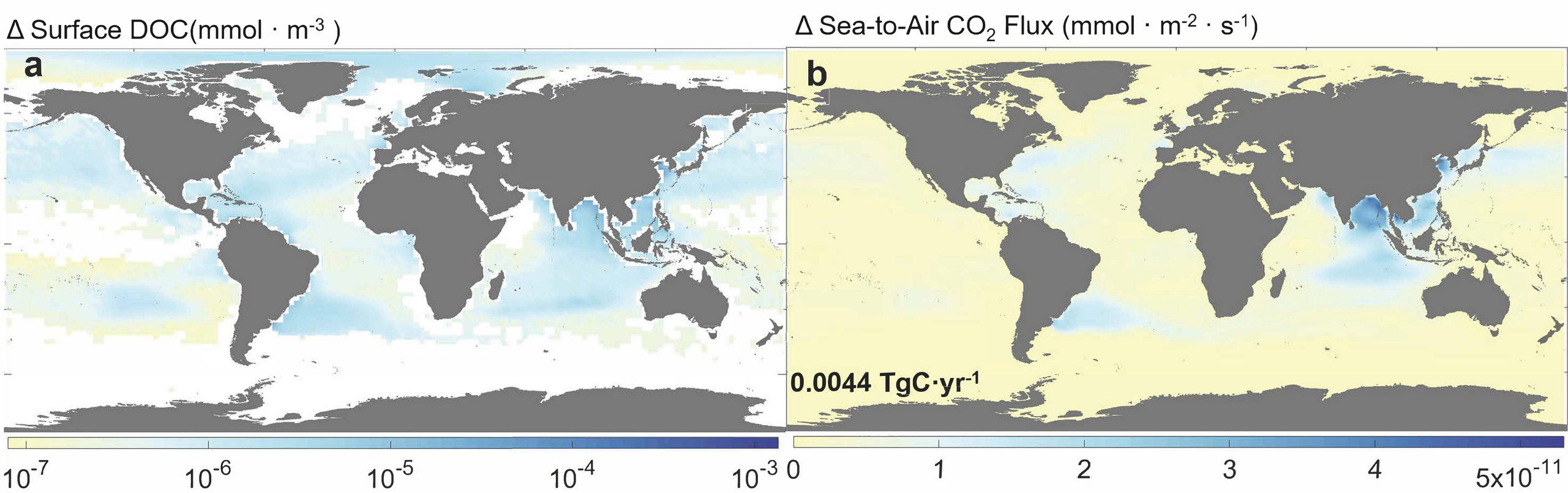
ABS

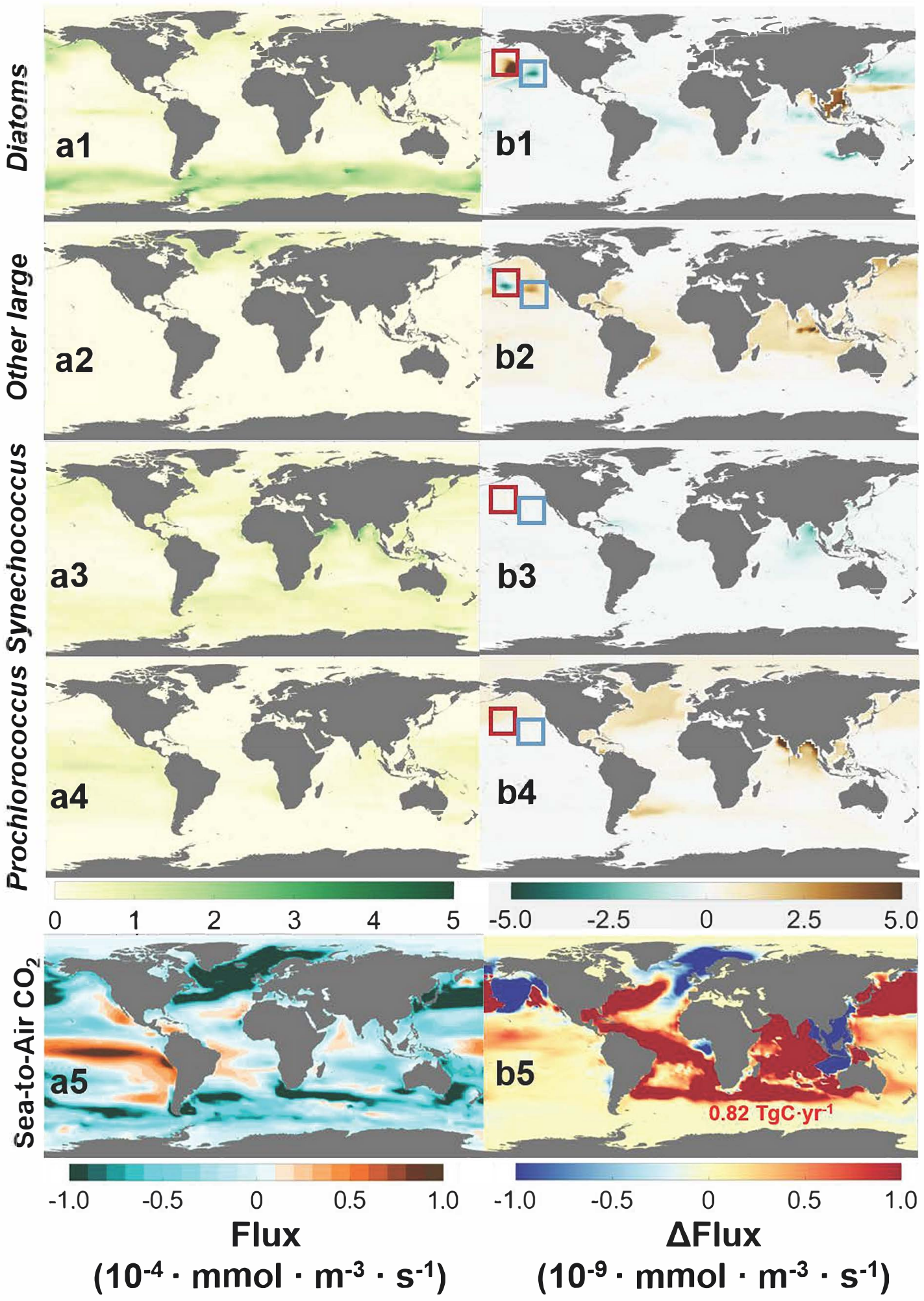
Depth (m)

10 100 1000 5000

Mass (Tg)

0 0.05 0.10 0.15 0.20


Δ Surface DOC(mmol · m-3)
a
Δ Sea-to-Air CO2 Flux (mmol · m-2 · s-1)
b
0.0044 TgC·yr-1
10-7
10-6
10-5
10-4
10-3
0
1
2
3
4
5x10-11


Plankton Growth (mmol C m-3)
ΔGrowth (%)
Diatoms
Other large
Synechococcus
Prochlorococcus
a1
b1
a2
b2
a3
b3
a4
b4
0 1 2 3 4 5
-5.0 -2.5 0 2.5 5.0
Sea-to-Air CO2
a5
b5
0.82 TgC·yr-1
-1.0 -0.5 0 0.5 1.0
-1.0 -0.5 0 0.5 1.0
Flux
(10-4 · mmol · m-3 · s-1)
ΔFlux
(10-9 · mmol · m-3 · s-1)